



Cite this: DOI: 10.1039/c6nj00401f

Accessible bidentate diol functionality within highly ordered composite periodic mesoporous organosilicas†

Lacey M. Reid,^a Gang Wu^a and Cathleen M. Crudden^{*ab}

Periodic mesoporous organosilica (PMO) materials containing methoxy- or methoxyethoxymethyl-ether protected biphenol dopants were synthesized and the protecting groups were cleaved to liberate reactive C₂-symmetric diols within the solid-state material. Treatment of the deprotected PMO materials with phosphoryl chloride yielded phosphate ester functional groups predominantly at the exposed biphenol sites, while protected materials showed only surface phosphate species. Since biphenols are closely related to common ligands for asymmetric catalysis, these results open up significant possibilities for the design of chiral recoverable catalysts with chiral groups embedded in the walls of the material.

Received (in Montpellier, France)
5th February 2016,
Accepted 11th May 2016

DOI: 10.1039/c6nj00401f

www.rsc.org/njc

Introduction

Periodic mesoporous organosilica (PMO) materials have fascinated materials and organic chemists for more than a decade since they are highly ordered combinations of organic cores and polymerized silicas. Due to the availability of monomers with highly stable C–Si bonds, organic and inorganic regions are perfectly separated, and when condensation is performed in the presence of surfactants, high-surface-area materials are produced with highly ordered arrays of pores.¹ These materials have been studied as prospective candidates for a wide variety of applications from catalysis and light-harvesting to chromatography and sensing, owing to their unique surface properties.^{1–3} In particular, manipulation of the central “R” unit in the bridged organosilane monomers [(R'O)₃Si–R–Si(OR')₃], is proposed as one of the most powerful aspects of these materials. However, in practice, few 100% PMO materials have been reported with any significant complexity in this R group, since complex central cores are known to disrupt ordering and stability of the material.^{1,4} This leads to the use of only low levels of complex organosilane dopant monomers that have little effect on the material, or to materials with poor order, in which case some of the key properties that make PMOs interesting are lost.

Several groups have reported the post-synthesis modification of organic bridging groups in PMOs can be used to introduce

functionality, for example, by sulfonation,⁵ Diels–Alder rearrangement,^{6,7} thiol–ene Click reaction⁸ or Friedel–Crafts alkylation⁹ of ethylene-bridged PMOs, or by modification of phenylene-bridged PMOs to yield amine^{10,11} or sulfonic acid^{12,13} functional groups. These new functional groups can be modified to yield even more complex organic functionality without sacrificing the high degree of order within the PMO material.^{5,14,15} While these reports describe efficient methods to achieve high loadings of functional groups, the original “R” organic backbone is limited to simple phenyl, alkyl or alkenyl groups rather than biaryls whose functionalization would be ideal to prepare two-coordinate complexes. And in many cases, controlling the positional selectivity of the post-synthesis modification is challenging.¹⁶

Herein we report a unique method for the preparation of well-defined, functional materials with high levels of functionality at specific sites. By preparing dopants monomers with protected functionality whose structures are designed to pack effectively with the bulk of the material, we are able to incorporate high levels of functional dopants in PMO materials without any loss of order. We then demonstrate, using traditional organic chemistry techniques, how reactive functional groups can be liberated after the material condensation is complete. Finally, we demonstrate that the liberated functional groups (diols) can be reacted in a second stage to produce precursors to catalytically active species. Through detailed CP MAS NMR studies, we show that diols can be selectively functionalized in the presence of surface silanols. Overall this work provides the first detailed assessment of the strategy of incorporated functionally active monomers in PMO materials without destruction of local or long-range order.

^a Department of Chemistry, Queen's University, Kingston, Ontario, K7L3N6, Canada. E-mail: cruddenc@chem.queensu.ca

^b Institute of Transformative Bio-Molecules (WPI-ITbM), Nagoya University, Nagoya 464-8602, Japan

† Electronic supplementary information (ESI) available: Additional solid-state NMR data and NMR characterization of PMO precursors. See DOI: 10.1039/c6nj00401f

Experimental

Materials and methods

All chemicals were purchased from Sigma Aldrich, TCI, Fisher Scientific or Acros Organics and used without further purification unless otherwise noted. Catalyst (1,5-cyclooctadiene)chlororhodium(II) dimer was generously provided by Johnson-Matthey. Anhydrous DMF was purchased from EMD Chemicals Inc. in a DrySolv container. Anhydrous ethanol was purchased from Commercial Alcohols and used without further treatment. Triethylamine and dichloro-methane were distilled over CaH₂ before use. THF and hexanes were distilled from sodium metal and benzophenone ketyl before use. Pyridine was distilled and stored over sodium hydroxide.

Solution NMR were recorded on a Bruker Avance 300 with a QXI probe (¹H: 300.1, ¹³C: 75.5 MHz), Bruker Avance 400 with a BBFO probe (¹H: 400.1, ¹³C: 101, ³¹P: 162 MHz) or Bruker Avance 500 with a BBFO probe (¹H: 500.0, ¹³C: 125.5 MHz). Shifts are reported in parts per million (ppm) with *J* coupling constants indicated in Hertz. ¹H and ¹³C spectra were calibrated from the solvent residual peak in CDCl₃ or DMSO-d₆ and ³¹P spectra were calibrated externally against 85% H₃PO₄ in water. Signal multiplicity is indicated by the abbreviations: s = singlet, d = doublet, t = triplet, q = quartet, m = multiplet.

Solid-state ¹³C, ²⁹Si and ³¹P NMR measurements were recorded on a Bruker Avance 600 NMR spectrometer using a Bruker 5 mm CP MAS probe, at a frequency of 151, 119 and 243 MHz, respectively. The ¹³C and ²⁹Si CP MAS spectra were referenced to adamantane, tetramethylsilane and ammonium dihydrogen phosphate, respectively. D1 delay time was 2 s for ¹³C and ²⁹Si spectra, and 3.5 s for ³¹P. The rotor was spun at a frequency of 10–12 kHz and the number of scans was typically 800–2000, 1000–2000, and 2000–4000 for ¹³C, ³¹P and ²⁹Si, respectively.

High-field ¹H MAS, ³¹P CP MAS and ³¹P-¹H HETCOR NMR experiments were run by Dr Victor V. Terskikh on a Bruker NMR (¹H = 899.8 MHz, ³¹P = 364.2 MHz) at the High-Field NMR Facility in Ottawa, Ontario, Canada. ¹H and ³¹P spectra were referenced to adamantane (10 kHz MAS) and ammonium dihydrogen phosphate, respectively, at 21.1 T using a 2.5 mm H/X MAS Bruker probe. ¹H MAS NMR spectra of PMO materials were recorded with a D1 delay time of 10 s with 90–90 rotor-sync echo, spinning at 20 kHz MAS for 32 scans. BINOL hydrogen phosphate reference spectra were recorded with a D1 delay time of 30 s with 16 scans. ³¹P MAS NMR spectra of PMO materials were recorded with direct polarization of phosphorous, H-P decoupled with a D1 delay time of 5 s and P1 width of 2 μs, spinning at 20 kHz for at least 6000 scans. ³¹P MAS NMR of BINOL hydrogen phosphate reference spectra were recorded with a D1 delay time of 30 s, P15 contact time of 5 ms, spinning at 20 kHz for 32 scans. ³¹P-¹H HETCOR of PMO samples were recorded with no homonuclear decoupling, with a D1 delay time of 3 s, P15 contact time of 500 μs, td2 × td1 = 1000 × 48, spinning at 20 kHz MAS for 2048 scans. ³¹P-¹H HETCOR of BINOL hydrogen phosphate reference spectra were recorded with a D1 delay time of 30 s, P15 contact time of 200 μs, td2 × td1 = 1000 × 192 with 8 scans collected (20 kHz MAS).

High-resolution mass spectroscopy analysis (HRMS) was performed by the Mass Spectroscopy and Proteomics Unit at Queen's University, Kingston, Ontario, Canada. Spectra were measured on a Micromass GCT GC-EI TOF mass spectrometer by EI⁺ fragmentation.

XRD analysis was performed using a SMART6000 2D detector equipped with a fixed chi, 3 circle goniometer, parallel beam optics, and Rigaku Cu rotating anode operating at 50 kV and 90 mA. Powder samples were loaded between Mylar films and spectra were corrected for Mylar background signals. Data was collected in transmission mode over two frames at 600 s each, at a measuring angle of a 2θ range of 1–40°. Measurements were recorded by the McMaster Analytical X-ray Diffraction Facility (MAX) in Hamilton, Canada.

TEM analysis was performed using a JEOL 2010 scanning transmission electron microscope operating at 200 keV. The powder sample, dispersed in ethanol, was dropped onto a porous carbon grid to fix the sample to the grid upon drying. The measurements were performed at Microscopy and Microanalysis facility at the University of New Brunswick, Fredericton, New Brunswick, Canada. Nitrogen adsorption experiments were performed using a Micromeritics ASAP 2010 physisorption analyser with nitrogen as the adsorbate gas. Powder samples were degassed at 80 °C for at least 8 hours before analysis.

Synthesis of organosilica monomers

Synthesis of precursor (6). The 4,4'-dinitro-2,2'-dimethoxy-1,1'-biphenyl **6** was prepared using a literature procedure, and spectral data for the prepared compound matched the reported characterization data.¹⁷ The product was used as prepared for the next step in the synthesis.

4,4'-Diamino-2,2'-dimethoxy-1,1'-biphenyl (7). Tin(II) chloride dihydrate (25.7 g) and the 2,2'-dimethoxy-4,4'-dinitro-1,1'-biphenyl **6** (3.45 g) were dissolved in anhydrous ethanol (120 mL) and the reaction was stirred for 24 h at 70 °C. The mixture was poured over crushed ice and the pH was adjusted to 7–8 with sodium bicarbonate. In a large separatory funnel, the thick aqueous mixture was gently agitated with ethyl acetate to extract the product. The organic phases were combined, washed with brine and dried over magnesium sulfate. Removal of the solvent *in vacuo* gave a light tan powder (2.63 g, 95% yield). The crude product matched the literature spectral data and was used in the next step without further purification. ¹H NMR (400 MHz, CDCl₃, δ ppm): 6.99 (d, 2H, *J* = 8.3 Hz), 6.31–6.29 (m, 4H), 3.70 (s, 6H), 3.68–3.59 (bs, 4H), ¹³C NMR (101 MHz, CDCl₃, δ ppm): 158.1, 146.7, 132.4, 118.3, 107.1, 99.1, 55.6. TOF HRMS (EI⁺) found 244.1204 *m/z* (calcd for C₁₄H₁₆N₂O₂: 244.1212).

4,4'-Diiodo-2,2'-dimethoxy-1,1'-biphenyl (8). Iodination of **7** was carried out according to a literature procedure.¹⁷ The product was obtained in 40% yield after purification by silica gel flash chromatography (98 : 2 petroleum ether : ethyl acetate) ¹H NMR (300 MHz, CDCl₃, δ ppm): 7.26 (dd, 2H, *J* = 7.9, 1.5 Hz), 7.19 (s, 2H), 6.84 (d, 2H, *J* = 6.8 Hz), 3.68 (s, 6H), ¹³C NMR (101 MHz, CDCl₃, δ ppm): 157.4, 132.6, 129.7, 126.5, 120.5, 93.6, 55.9. TOF HRMS (EI) *m/z*: [M + H]⁺ calcd for C₁₄H₁₂I₂O₂: 465.8927; found 465.8939 *m/z*.

4,4'-Diiodo-2,2'-dihydroxy-1,1'-biphenyl (9). Compound **8** (1.33 g) was dissolved in dry dichloromethane (5.8 mL) in a flame-dried 50 mL round-bottom flask under argon gas. The solution was cooled to $-78\text{ }^{\circ}\text{C}$ and a 1 M solution of BBr_3 in dichloromethane (8.6 mL) was added cautiously. The reaction was held at $-78\text{ }^{\circ}\text{C}$ for 2 h then allowed to warm to room temperature overnight. The flask was placed on ice and the reaction was quenched slowly with methanol and subsequently diluted with distilled water. Aqueous sodium thiosulfate was added and the product was extracted with ethyl acetate. The combined organic phases were washed with aqueous sodium thiosulfate, water and brine, and dried over magnesium sulfate. The solvent was removed *in vacuo* to give a tan powder. The crude was recrystallized with ethyl acetate/hexanes (1 : 1) to give fluffy off-white needles (723 mg, 58% yield). ^1H NMR (300 MHz, CDCl_3 , δ ppm): 7.41 (d, 4H, 7.2 Hz), 6.97 (d, 2H, 8.1 Hz). ^1H NMR (300 MHz, DMSO-d_6 , δ ppm): 9.66 (s, 2H), 7.23 (d, 2H, $J = 1.7$ Hz), 7.16 (dd, 2H, $J = 8.0$ Hz, 1.7 Hz), 6.89 (d, 2H, $J = 1.7$ Hz). ^{13}C NMR (101 MHz, DMSO-d_6 , δ ppm): 156.2, 133.5, 127.8, 125.1, 124.8, 93.7. TOF HRMS (EI) m/z : $[\text{M} + \text{H}]^+$ calcd for $\text{C}_{12}\text{H}_8\text{I}_2\text{O}_2$: 437.8614; found 437.8619 m/z .

4,4'-Diiodo-2,2'-di(2-methoxyethoxymethyl)-1,1'-biphenyl (10). Compound **9** (888 mg) was dissolved in THF (10 mL) in a dried 50 mL round-bottom flask under argon. The flask was cooled to $0\text{ }^{\circ}\text{C}$ in an ice bath. NaH 60% in mineral oil was weighed out (490 mg) and added to the reaction by quickly removing the rubber septum. The mixture bubbled vigorously and the yellow suspension became a tan slurry. The mixture was stirred for 1 hour at $0\text{ }^{\circ}\text{C}$ and another portion of NaH in mineral oil (100 mg) was added. MEMCl was subsequently added dropwise at $0\text{ }^{\circ}\text{C}$ and the reaction was allowed to slowly warm to room temperature. After 18 h the reaction was quenched dropwise with water. When the mixture ceased bubbling it was diluted with water and ethyl acetate. The aqueous phase was extracted with ethyl acetate and the combined organic phases were washed with brine and dried over sodium sulfate. The solution was concentrated under vacuum to a volume of ~ 1 mL and then loaded onto a silica gel column. The crude was purified by flash chromatography (3 : 1 petroleum ether : ethyl acetate) to yield the product as a yellow oil (724 mg, 58%). ^1H NMR (400 MHz, CDCl_3 , δ ppm): 7.61 (d, 2H, $J = 1.6$ Hz), 7.41 (dd, 2H, $J = 8.0$ Hz, 1.6 Hz), 6.91 (d, 2H, $J = 8.0$ Hz), 5.15 (s, 4H), 3.69 (AA'BB', 4H), 3.52 (AA'BB', 4H), 3.40 (s, 6H). ^{13}C NMR (101 MHz, CDCl_3 , δ ppm): 155.3, 132.5, 131.1, 127.7, 124.6, 94.2, 93.4, 71.5, 67.8, 59.1. TOF HRMS (EI) m/z : $[\text{M} + \text{H}]^+$ calcd for $\text{C}_{20}\text{H}_{24}\text{I}_2\text{O}_6$: 613.9662; found 613.9650 m/z .

4,4'-Bis(triethoxysilyl)-2,2'-dimethoxy-1,1'-biphenyl (2). Compound **8** (218 mg), chloro(1,5-cyclooctadiene)rhodium(i) dimer catalyst (10 mol%, 33 mg) and tetrabutylammonium iodide (330 mg) solids were dissolved in anhydrous DMF (2.3 mL) in a dried, 20 mL glass vial under argon flow. Cyclooctadiene (0.06 mL), triethoxysilane (0.34 mL) and triethylamine (0.39 mL) were added by syringe through the rubber septum capping the vial. The septum was quickly replaced with a Teflon-lined lid and the capped vial was heated to $80\text{ }^{\circ}\text{C}$ for 48 hours. The solvent and excess volatile reagents were removed by Kugel Rohr distillation at

$80\text{ }^{\circ}\text{C}$ under high-vacuum. The brown residue was triturated with diethyl ether (3×5 mL) and these combined volumes were concentrated down to ~ 0.5 mL and loaded onto a silica gel column. The product was purified by flash chromatography (7 : 1 petroleum ether : ethyl acetate) to give a yellow oil (113 mg, 45% yield). By ^1H NMR spectroscopy, the product contained a small amount of mono-silylated monomer that could not be removed. The product was carried on to materials synthesis. ^1H NMR (300 MHz, CDCl_3 , δ ppm): 7.34–7.27 (m, 6H), 3.94 (q, 12H, $J = 7.0$ Hz), 3.81 (s, 6H), 1.30 (t, 18H, $J = 7.0$ Hz), ^{13}C NMR (75.5 MHz, CDCl_3 , δ ppm): 156.5, 131.3, 131.1, 129.9, 127.0, 117.0, 59.2, 55.7, 18.3. TOF HRMS (EI) m/z : $[\text{M} + \text{H}]^+$ calcd for $\text{C}_{26}\text{H}_{42}\text{O}_8\text{Si}_2$: 538.2418; found 538.2433 m/z .

4,4'-Bis(triethoxysilyl)-2,2'-di(2-methoxyethoxymethyl)-1,1'-biphenyl (3). The bis-iodo compound **10** was prepared using identical conditions to the dimethoxy monomer **2**. The brown residue remaining after Kugel Rohr distillation was triturated with THF and these combined fractions were concentrated and loaded onto a silica gel column. The product was purified by flash chromatography (1 : 1 petroleum ether : ethyl acetate) to give a yellow oil in 41% yield. ^1H NMR (400 MHz, CDCl_3 , δ ppm): 7.51 (s, 2H), 7.38 (dd, 2H, $J = 7.5$ Hz, 0.9 Hz), 7.27 (d, 2H, $J = 7.5$ Hz), 5.16 (s, 4H), 3.93 (q, 12H, $J = 7.0$ Hz), 3.63 (AA'BB', 4H, $J = 12.1$ Hz, 5.7 Hz, 3.8 Hz), 3.46 (AA'BB', 4H, $J = 12.1$ Hz, 5.7 Hz, 3.8 Hz), 3.53 (s, 6H), 1.30 (t, 18H, $J = 7.0$ Hz), ^{13}C NMR (101 MHz, CDCl_3 , δ ppm): 154.47, 131.75, 131.36, 131.03, 128.39, 121.84, 94.50, 71.56, 67.53, 58.96, 58.82, 18.27. TOF HRMS (EI) m/z : $[\text{M} + \text{H}]^+$ calcd for $\text{C}_{32}\text{H}_{54}\text{O}_{12}\text{Si}_2$: 686.3154; found 686.3145 m/z .

4,4'-Diiodo-1,1'-biphenyl-2,2'-diyl hydrogen phosphate. The bis-iodo compound **9** (100 mg) was dissolved in dry pyridine (0.5 mL) in a dried 3 mL vial purged with argon gas. Phosphoryl chloride (0.05 mL, 2 eq.) was added at room temperature and the vial was sealed with a Teflon-lined cap and heated to $80\text{ }^{\circ}\text{C}$. The clouded mixture gradually became a clear dark amber solution. After 4 h stirring at $80\text{ }^{\circ}\text{C}$, the reaction was cooled and the vial placed on ice. Distilled water was added cautiously (0.2 mL) and vigorous bubbling was observed. When bubbling had ceased, the vial was capped and heating at $80\text{ }^{\circ}\text{C}$ was resumed. The reaction was stirred for 48 h then cooled and diluted with ethyl acetate and poured into dilute HCl. The aqueous phase was extracted with ethyl acetate until clear. The combined organic phase was dried over sodium sulfate and the solvent was removed *in vacuo* to give an off-white solid that was triturated with dichloromethane. Recrystallization of the solid with 1 : 1 ethyl acetate/methanol gave a tan solid (33 mg). ^1H NMR (400 MHz, DMSO-d_6 , δ ppm): 7.72 (d, 2H, $J = 7.6$ Hz), 7.58 (s, 2H), 7.37 (d, 2H, $J = 7.9$ Hz). ^{13}C NMR (101 MHz, DMSO-d_6 , δ ppm): 134.9, 131.5, 130.6, 128.3, 95.6. ^{31}P NMR (162 MHz, DMSO-d_6 , δ ppm): 3.34.

General procedure for synthesis of PMO materials

Materials were prepared according to a reported procedure for biphenylene-bridged PMO materials.¹⁸ In a typical procedure, a mixture of the organosilane precursor **2** or **3** with bulk monomer 1,4-bis(triethoxysilyl)biphenyl (BTESBP) **1**, was added dropwise to a stirring alkaline solution (0.51 M aq. NaOH) of

octadecyltrimethylammonium chloride surfactant (1.3 eq. to total organosilane) at room temperature. The sol was stirred at room temperature for 24 hours at 600 rpm, then subjected to static aging at 95 °C for 24 hours. The white solid was collected by vacuum filtration and washed with several portions of distilled water. The surfactant template was removed by stirring the powder in either ethanol or acidic ethanol (0.05 M in HCl) at 60 °C. The powder was again collected by vacuum filtration and washed with ethanol, then dried overnight in a vacuum oven at 80 °C.

To passivate the surface of the PMO materials, the solid was suspended in dry hexanes (50 g L⁻¹) and hexamethyl-disilazane (0.003 L g⁻¹ PMO) was added dropwise to the stirring solution at room temperature. The suspension was heated to 65 °C for 18 h and then cooled down and filtered over vacuum. The powder was washed with ethyl acetate, anhydrous ethanol and then acetone before being dried overnight at 80 °C under vacuum to give the TMS-capped PMO.

Deprotection of PMO materials

Methoxy ether deprotection of solid-state materials was achieved with boron tribromide. The PMO material (40 mg) was suspended in dry dichloromethane (1.5 mL) and cooled to -78 °C. A solution of BBr₃ 1 M in dichloromethane (1.5 mL) was added dropwise and the suspension was stirred for a further 2 hours at -78 °C before slowly warming to room temperature. After 48 hours, the reaction was quenched with distilled water and the material was collected by vacuum filtration. The powder was washed with sodium thiosulfate, water, and ethanol, before being dried overnight at 80 °C under vacuum to recover 34 mg white powder.

For deprotection of MEMO-PMOs, the solid-state material (47 mg) was suspended in 15 mL acidified ethanol (0.05 M in HCl) and stirred for 24 h at 60 °C. The solids were filtered over vacuum and washed with ethanol then dried at 80 °C under vacuum to give 31 mg PMO.

General procedure for preparation of phosphate ester PMOs

PMO solids (40–50 mg) were suspended in dry pyridine (~1 mL) in a dried 3 mL vial purged with argon. Phosphoryl chloride (0.05–0.1 mL) was added at room temperature. The suspension was stirred at room temperature or 80 °C for 18–24 h before cooling to 0 °C in an ice bath and quenching by a few drops of distilled water. When the bubbling had ceased, the PMOs were left to stir for 9 h at room temperature after which they were diluted with distilled water. The materials were filtered by vacuum, washing with 2 M HCl, water, ethanol and ethyl acetate, then dried overnight at 80 °C under vacuum. PMOs withstood the treatment in pyridine at 80 °C without any degradation, but the reaction proceeded to the same degree at room temperature over 24 h by ³¹P NMR, therefore the reported data of HOP(O)-PMOs herein describe materials treated with POCl₃ at room temperature.

To determine extent of phosphate ester cleavage, the HOP(O)-PMO was suspended in 2 M HCl and stirred at room temperature for 18 h before filtering over vacuum and washing

with distilled water, ethanol and ethyl acetate. The material was dried at 80 °C under vacuum.

Mesoporous silica MCM-41 was prepared from tetraethyl-orthosilicate (10.5 mL) added to a stirring solution of C₁₆TAB surfactant (2.4 g) and 30% ammonium hydroxide (10.5 mL) in distilled water (120 mL). The sol was stirred for 2 hours at room temperature then filtered over vacuum, washing with distilled water. The material was dried for 24 h at 80 °C under vacuum before further treatment.

The MCM-41 (40 mg) was suspended in dry pyridine (0.7 mL) in a dried 3 mL vial purged with argon gas, then phosphoryl chloride (0.12 mL) was added at room temperature. The vial was sealed with a Teflon-lined cap and the reaction stirred for 1 hour at room temperature. After 1 h the reaction was cooled on ice and quenched cautiously with a few drops of distilled water, then continued to stir at room temperature for 4 h before the solid was filtered over vacuum and washed with distilled water and ethyl acetate. The powder was dried overnight at 80 °C under vacuum to give the HOP(O)-material as a white powder (35 mg).

HOP(O)-MCM was suspended in 2 M HCl and stirred at room temperature for 18 h before filtering over vacuum and washing with 2 M HCl, distilled water, then ethyl acetate. The material was recovered as a white solid (30 mg) after drying overnight at 80 °C under vacuum.

Results and discussion

PMO materials functionalized with a biphenol-type dopant

In ground breaking work, Inagaki and co-workers have shown that simple aromatic monomers such as bis(triethoxysilyl)-biphenyl (BTESBp, **1**) can form highly ordered materials with crystal-like ordering of the monomers within the PMO pore walls.¹⁸ These unique structures may result in interesting surface properties including confinement effects that would be advantageous in catalysis.¹⁹

Structurally related biphenols and binaphthols are widely employed as ligands for metal-catalyzed reactions^{20,21} and thus we chose to prepare protected versions of these ligands and attempt their incorporation in crystalline¹⁸ BTESBp (**1**)-based PMOs. We anticipated that removal of the ether protecting groups would be readily accomplished post-synthesis to generate reactive diols (Fig. 1). The reactivity of the liberated C₂-symmetric diol would then be tested by the formation of a phosphate ester.²²

Functional monomers **2** and **3** were thus targeted as precursors to the final deprotected biphenol species. In **2**, the phenol functional groups are protected as methyl ethers, chosen for their small size to be minimally disruptive to the crystal-like ordering of the PMO pore walls. Monomer **3**, bearing a methoxy-ethoxymethyl ether (MEM) substituent, was also prepared since this protecting group is typically removed under milder conditions than the simple methyl ether in **2**. The synthesis of both monomers begins with commercially available precursor **4** through modification of a known route to 4,4'-diiodo-2,2'-dimethoxy-1,1'-biphenyl **8** (Scheme 1).¹⁷ From **8**, MEM-protected precursor **10**

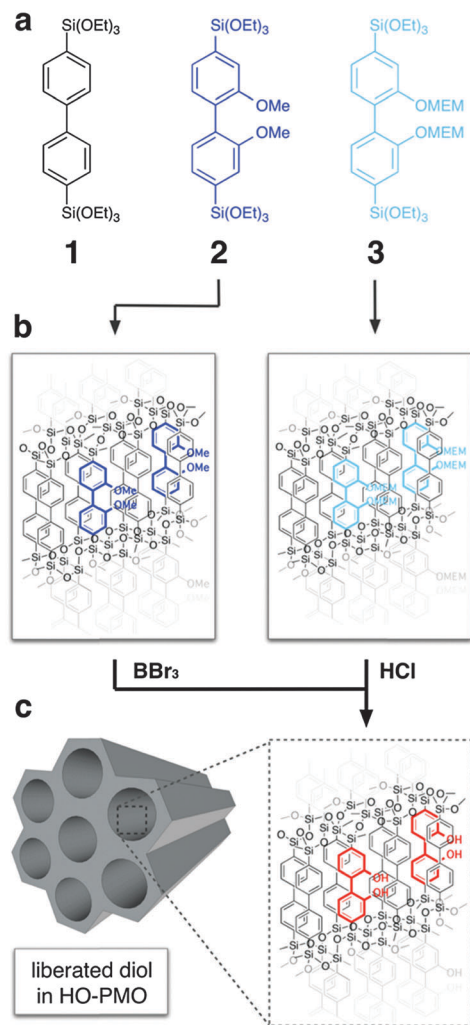
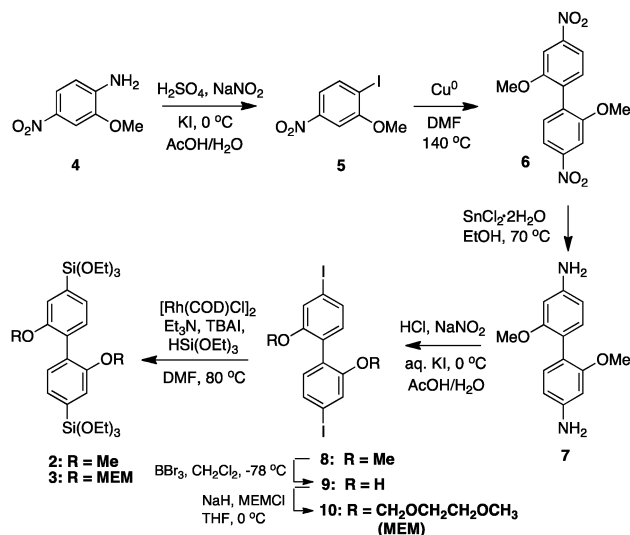


Fig. 1 (a) Functional monomers are combined with BTESBP 1 to prepare (b) PMO materials with dopants embedded in the pore walls; (c) removal of protecting groups liberates the free biphenol functionality within the solid-state PMO. MEM = methoxyethoxymethyl.

could be obtained in two steps. The final silylated monomers 2 and 3 were prepared by rhodium-catalyzed cross-coupling of the respective bis-iodo precursor 8 or 10 with triethoxysilane.²³

PMO materials were then prepared *via* base-catalyzed co-condensation of bulk monomer 1 and dopant 2 or 3 at up to 30% loading, employing an alkylammonium surfactant as the structure-directing agent according to the method previously described for biphenylene-bridged PMOs.¹⁸ A mild solution extraction with ethanol at 60 °C was employed to remove the templating surfactant. This procedure was used to prepare composite PMOs (cPMOs) named ^XMeO- and ^XMEMO-cPMOs, where *X* is the mol% loading of dopant 2 or 3, respectively. These materials exhibited mesoporous capillary condensation isotherms with average pore sizes of approximately 21 Å, similar to 100% BTESBP materials (Table 1). Surface areas in the doped materials were typically slightly lower compared to PMOs prepared solely from BTESBP, indicating small morphological changes within the PMO, however pore sizes



Scheme 1 Synthesis of methoxy- and MEM-protected monomers.

Table 1 Surface area (SA), pore diameter (*D_p*) and pore volume (*V_p*) characterization of PMO materials doped with 2 or 3. Dopants are expressed in molar% by formulation

BTESBP 1 bulk monomer + 2 or 3 (10-30 mol%) $\xrightarrow[\text{NaOH, H}_2\text{O}]{\text{C}_{18}\text{TMACl}}$ composite PMO MeO-cPMO or MEMO-cPMO

PMO	Dopant (mol%)	SA ^a (m ² g ⁻¹)	<i>D_p</i> ^b (Å)	<i>V_p</i> ^c (cm ³ g ⁻¹)
100%-BTESBP-PMO	(0)	711	20.5	0.521
¹⁰ MeO-cPMO	2 (10)	591	20.6	0.407
²⁰ MeO-cPMO	2 (20)	647	20.7	0.421
³⁰ MeO-cPMO	2 (30)	631	20.6	0.433
¹⁰ MEMO-cPMO	3 (10)	723	20.4	0.628
²⁰ MEMO-cPMO	3 (20)	636	19.2	0.499
³⁰ MEMO-cPMO	3 (30)	764	19.3	0.613

^a Calculated from BET isotherm. ^b Calculated by BJH method. ^c Single point total pore volume at *P/P*₀ 0.9999 mmHg.

remained virtually identical to the parent PMO material, even up to 30% loading of the functional monomer.

Incorporation of dimethoxybiphenyl monomer 2 in the composite PMO (cPMO) was confirmed by solid-state ¹³C cross-polarization magic angle spinning (CP MAS) NMR of the solid powders. In addition to resonances at *ca.* 135 ppm due to aromatic carbons in both dopant and bulk monomers, signals at 52 and 156 ppm representing the O-CH₃ and (Ar)C-O carbons were observed, increasing in magnitude as the loading of the dopant in the PMO material increased (Fig. 2a).

MeO-cPMOs showed a high degree of monomer condensation with the major ²⁹Si signals representing T₂ (R-SiO₂OH) and T₃ (R-SiO₃) sites (Fig. 2b). The integrity of the organosilane monomers was preserved in all of the cPMO materials, as confirmed by the lack of ²⁹Si CP MAS NMR signals at -100 ppm (Q-sites) that would indicate Si-C bond cleavage (Fig. 2b).

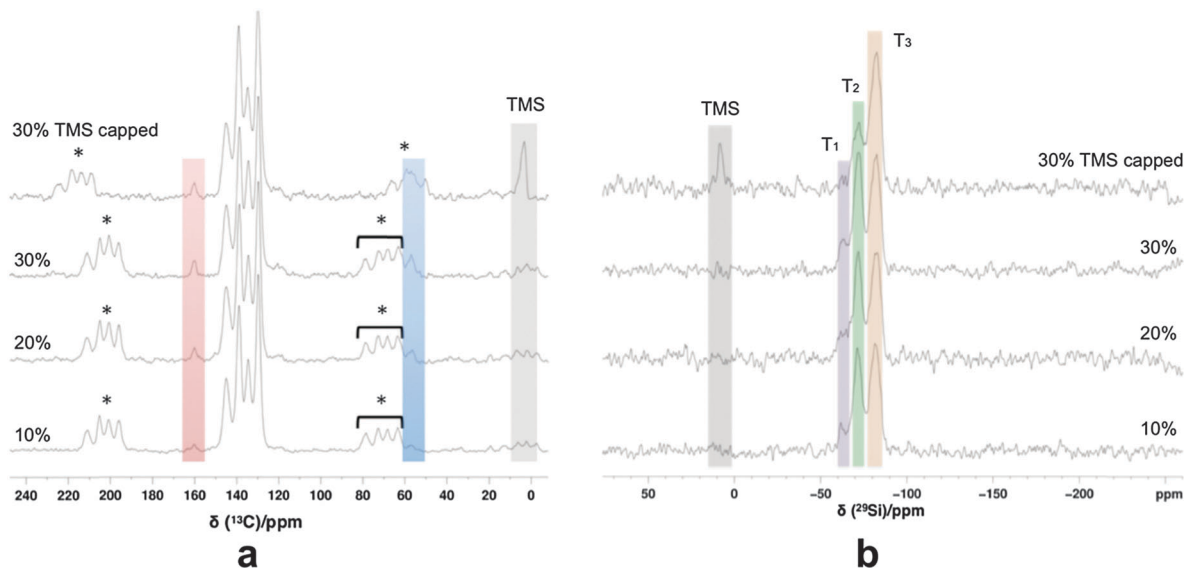


Fig. 2 Solid-state (a) ^{13}C and (b) ^{29}Si CP MAS NMR of doped MeO-cPMO materials, with MAS side bands indicated with an asterisk (*).

Solid-state NMR also confirmed passivation of surface silanols after treatment with hexamethyldisilazane, which was employed prior to cleavage of the methoxy ether protecting groups (Fig. 2a and b).[‡] The surface trimethylsilyl groups were visible at -1 ppm in the solid-state ^{13}C NMR, and the corresponding ^{29}Si signal for the silicon environment of TMS appeared at 5 ppm.

The MeO-functionalized cPMO materials retained a high degree of order in the pore walls even at high dopant loadings. In addition to the parent signal at $2\theta = 1.98$ due to the 45 \AA d_{100} spacing of the hexagonally ordered mesopores, powder X-ray diffraction (pXRD) analysis in the medium-angle region showed strong signals at d spacings of 11.8, 5.92, 3.95, 2.96 and 2.37 \AA (Fig. 3a). These higher order reflections indicate a lamellar ordering of monomers in a crystal-like lattice within the pore walls with a molecular spacing of $d = 11.8 \text{ \AA}$ ($2\theta = 7.48$), corresponding to the length of the bridging biphenylene unit. This is in agreement with previously reported 100% biphenylene-bridged PMOs.¹⁸ Remarkably, composite PMO materials prepared with 30 mol% of dopant 2 showed no change in the number or intensity of higher order diffraction peaks consistent with long range ordering,[§] suggesting that the dopant does not disrupt the highly ordered structure of the parent biphenylene-bridged PMO. Attempts to reach even higher loadings of 2 resulted in no polycondensation and precipitation of the PMO solid from solution.

The MeO-cPMO materials showed Type-IV nitrogen adsorption isotherms similar to 100% BTESBp PMOs, and displayed isotherms characteristic of ordered porous materials even at 30 mol% loading of dopant 2 (Fig. 3b). The distribution of pore

sizes was calculated from the adsorption isotherm data using the Barrett-Joyner-Halenda model and showed remarkably similar pore sizes for all doped materials, at $20 \pm 0.7 \text{ \AA}$.

Transmission electron microscopy (TEM) images of the MeO-cPMOs were similar for both 20%- and 30%-doped materials. While the layering of the thick, amorphous particles tended to obscure the mesoscopic ordering patterns by TEM, images focused on the thinner edges of particles clearly show 2D hexagonal packing of mesopores (Fig. 3c and d).

A related series of MEMO-cPMO materials were prepared by doping 10–30% of monomer 3 into BTESBp. Surprisingly, the longer-chain MEM protecting groups were also well tolerated and showed no disruption to long-range ordering of the monomers in cPMO materials at up to 30% of the MEMO dopant by formulation[§] (Fig. 4a). The MEMO-cPMOs displayed high surface areas of $> 600 \text{ m}^2 \text{ g}^{-1}$ with pore diameters of 19 \AA (Fig. 4b), which are slightly smaller than the MeO-cPMOs. As the dopant loading was increased across the set of cPMO materials, similar to the MeO-cPMO materials, no large differences were observed at different loadings of dopant, consistent with the fact that these dopants are not disruptive to the overall structure of the material (Table 1 and Fig. 4b).

Deprotection within the PMO: accessing the free biphenol

With several families of highly ordered BTESBp PMO materials doped with 2 or 3 in hand, the next step was to cleave the methoxy or MEM ethers to liberate free diol groups within the material. Deprotection of the MeO-cPMOs to produce the corresponding HO-cPMO materials was carried out with boron tribromide (BBr_3) under conditions typically used for the deprotection of simple organic compounds.²⁴ Despite the relatively harsh conditions, the composite PMO materials were stable during deprotection, showing no indication of decomposition in the solid-state ^{29}Si NMR spectra (Fig. S1, ESI[†]). Solid-state ^{13}C NMR spectra were recorded before and after treatment of the material to investigate the extent of deprotection (Fig. 5a). The aliphatic

[‡] TMS-passivation of the surface was not a requirement for the deprotection, but a larger excess of boron tribromide (up to 10 eq.) was necessary without passivation.

[§] Actual incorporation of the dopant within the materials can be roughly estimated by line fitting of solid-state ^{13}C NMR data. These are not without notable errors. See ESI[†] for details.

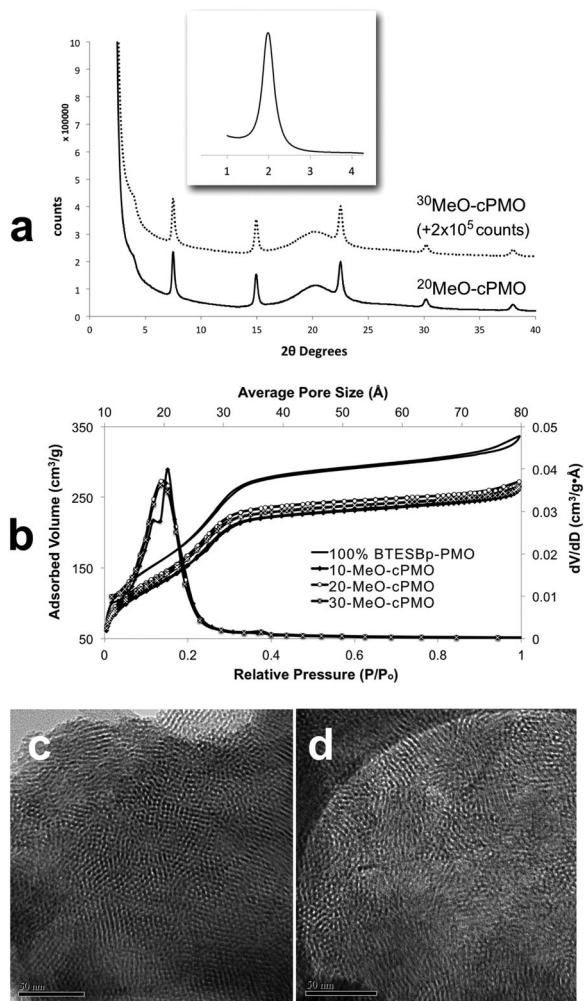


Fig. 3 (a) Medium and (inset) small angle XRD diffractogram of MeO-cPMOs, with the diffractogram for $^{30}\text{MeO-cPMO}$ offset by 200 000 counts for ease of viewing; (b) nitrogen adsorption isotherms and pore size distributions for MeO-cPMOs; and TEM images of (c) $^{20}\text{MeO-cPMO}$ and (d) $^{30}\text{MeO-cPMO}$ with scale bar indicating 50 nm.

peak at 52 ppm originating from the methoxy carbon decreased significantly after the deprotection. The aromatic carbon signal at 156 ppm was observed to shift upfield to 152 ppm as the free hydroxyl group was liberated. However, even treatment with a large excess of boron tribromide over 48 hours at room temperature, did not result in complete deprotection of all methoxy groups. These remaining protected monomers can be observed in the solid-state ^{13}C NMR as residual peaks at 52 and 156 ppm, however it is clear that a large number of methoxy groups have been removed by the process.

Passivation of the cPMO surface with trimethylsilyl groups prior to the Lewis-acid assisted deprotection was also examined, and also showed residual signals from the methoxy-protected monomer (Fig. S1, ESI[†]). Repeated treatment of the deprotected PMO under the same conditions did not appear to promote further deprotection, suggesting that some dopant monomers are buried within the organosilica framework and are not accessible to BBr_3 .

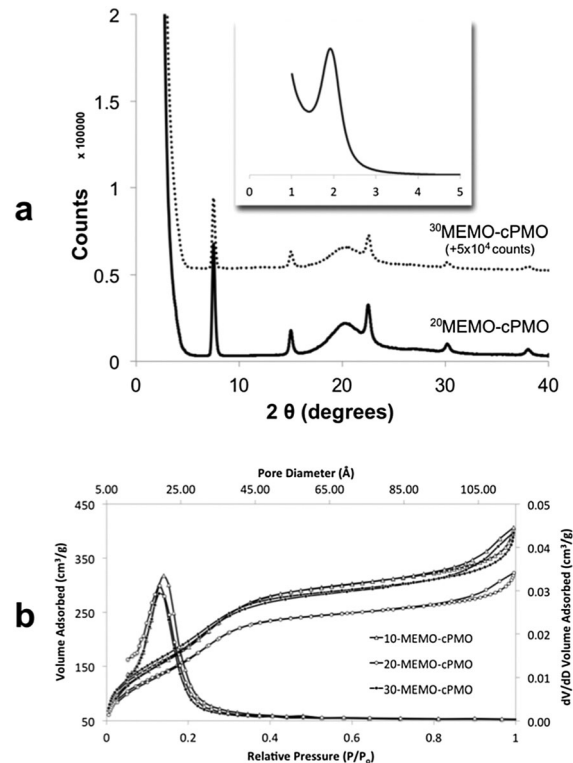


Fig. 4 (a) Medium and (inset) small angle XRD diffractogram of PMOs with 20% and 30% dopant loadings of monomer **3**, with the diffractogram for $^{30}\text{MEMO-cPMO}$ offset by 50 000 counts for ease of viewing; (b) nitrogen adsorption isotherms and pore size distributions of MEMO-cPMO materials.

Although there have been some reports of apparently complete deprotection of embedded methyl ethers,²⁵ typically more easily removed protecting groups need to be employed,^{26,27} and it is often observed that some embedded protecting groups are never removed, a factor likely dependent on morphology.⁹

As expected, removal of the MEM groups could be affected under milder conditions than those required with the methyl ether: considerable cleavage was even observed during acidic extraction of the surfactant from the PMO pores (Fig. S2, ESI[†]), and prolonged heating in the presence of acidic ethanol allowed the majority of the MEM groups to be deprotected *in situ*.

Fig. 5b shows the solid-state ^{13}C NMR profile of a $^{20}\text{MEMO-cPMO}$ material first treated with pure ethanol to remove the surfactant, and then with acidified ethanol to cleave the MEM ether groups to give hydroxyl functionalized materials (HO-cPMO).[†] As observed with the MeO-cPMO materials, a small proportion of inaccessible MEM groups were observed, as evidenced by the small aliphatic signals at 67 and 70 ppm shown in Fig. 5b. Larger signals at 15 and 57 ppm are thought to come from the byproducts of the MEM hydrolysis that may also become trapped in the organosilica matrix.

Interestingly, in the case of the MEMO-cPMOs, TMS-passivation actually hindered the deprotection, possibly by

[†] Due to the weaker ability of neutral ethanol as an extraction solvent, some surfactant is still observed in the pores.

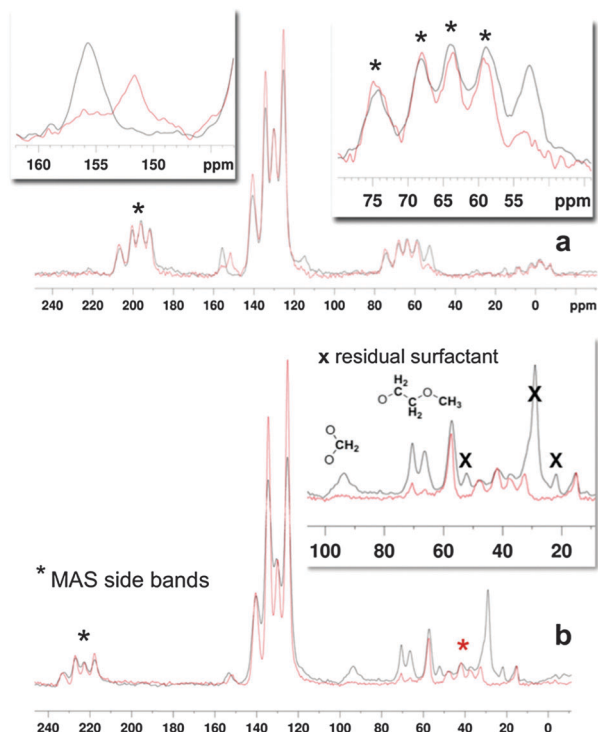


Fig. 5 Solid-state ^{13}C CP MAS NMR spectra of (a) $^{30}\text{MeO-cPMO}$ with zoomed aromatic (inset, left) and aliphatic (inset, right) regions, and; (b) $^{20}\text{MEMO-cPMO}$ with zoomed aliphatic region (inset), before (black) and after (red) deprotection of the dopant with boron tribromide or acid, respectively, with MAS side bands and residual surfactant signals \ddagger indicated.

increasing the hydrophobicity of the surface, which then would hinder interactions between the ethanolic solution and the PMO pores. Similar to the case of passivated MeO-cPMO materials, the introduction of TMS groups coating the surface generally resulted in decreased pore size and pore volume (Table 2). Because of the increased hydrophobicity, the MEM groups remained intact after treatment with the acidified ethanol for 6 hours at 55 °C, but could be cleaved under the same conditions over several days (Fig. S3, ESI \dagger). \parallel The facile removal of the MEM groups under mildly acidic conditions makes the MEM dopant a convenient and practical precursor to the biphenol moiety inside PMO materials. The monomer can even be deprotected in a single step during the surfactant extraction.

Having liberated the free biphenol moiety from both MeO- and MEMO-cPMO materials, it was then critical to determine whether the diol group could be further manipulated within the HO-cPMO framework. Preparation of hydrogen phosphate ester derivatives from biphenol- and BINOL-type compounds is synthetically straightforward and can be corroborated by ^{31}P NMR. 28,29 Furthermore, phosphate ester derivatives have been reported recently as Brønsted acid catalysts for a variety of interesting transformations, $^{29-32}$ and related phosphoramidates are highly effective ligands for asymmetric catalysis. 32,33

\parallel Prolonged acidic treatment also removed the surface TMS groups. The MEMO-PMOs were not subjected to the harsher boron tribromide deprotection conditions.

Table 2 Surface area (SA), pore diameter (D_p) and pore volume (V_p) characterization of surface-passivated and deprotected PMO materials prepared with dopant **2** or **3**. Dopants are expressed in molar% by formulation

PMO	Dopant (mol%)	SA ^a (m ² g ⁻¹)	D_p^b (Å)	V_p^c (cm ³ g ⁻¹)
$^{20}\text{MeO-cPMO-TMS}^d$	2 (20)	858	17.4	0.522
$^{30}\text{MeO-cPMO-TMS}^d$	2 (30)	716	17.4	0.495
$^{30}\text{MeO-cPMO-TMS}^{d,e}$	2 (30)	712	17.7	0.401
$^{20}\text{MEMO-cPMO}$	3 (20)	738	19.1	0.452
$^{30}\text{MEMO-cPMO}$	3 (30)	755	19.2	0.447
$^{20}\text{MEMO-cPMO-H}^f$	3 (20)	710	19.3	0.506
$^{20}\text{MEMO-cPMO-H}^{d,f}$	3 (20)	777	18.8	0.489

^a Calculated from BET isotherm. ^b Calculated by BJH method. ^c Single point total pore volume at P/P_0 0.9999 mmHg. ^d TMS-passivated PMO materials. ^e Treated with boron tribromide. ^f Treated with acidified ethanol.

To prepare supported organophosphate derivatives, deprotected materials were suspended in pyridine and treated with phosphoryl chloride (POCl_3) overnight at room temperature before quenching the reaction with water to produce the hydrogen phosphate derivative **11** (Fig. 6). The reaction mixture was filtered and excess reagents were further removed by washing successively with 2 M HCl, distilled water, ethanol, and organic solvent. The resultant PMO powders were dried under vacuum to give the corresponding HOP(O)-cPMOs, which showed no loss of material integrity by ^{29}Si NMR (Fig. S4, ESI \dagger).

As seen in Fig. 6a and b, the solid-state ^{31}P NMR spectra of HOP(O)-cPMOs exhibit a strong signal at 0 ppm. This ^{31}P chemical shift is comparable to the analogous organophosphate diester **11** prepared from the iodo-precursor **9**, whose ^{31}P signal was observed at 3.3 ppm in solution (see ESI \dagger). The ^{31}P spectra also showed a small shoulder at about -10 ppm as well as a small, broad signal at -22 ppm. The identities of these additional signals were investigated by control experiments described below.

Subjecting a MeO-cPMO material to phosphoryl chloride before deprotection resulted in major ^{31}P signals at -10 and -22 ppm and a minor signal at 0 ppm (Fig. 6c). Previous ^{31}P NMR studies on silicophosphate glasses, xerogels and porous materials have reported Si-O-P resonances at -10 and -24 ppm for phosphate species $[\text{O} = \text{P}(\text{OSi})(\text{OH})_2]$ and $[\text{O} = \text{P}(\text{OSi})_2(\text{OH})]$, respectively. $^{34-37}$ In support of this assignment, these signals were also observed in a 100%-BTESBp-derived PMO material subjected to phosphoryl chloride under identical conditions (Fig. 6d). Thus it is likely that these signals originate from surface phosphate esters resulting from the reaction of phosphoryl chloride with exposed silanols. However, these 'non-diol' materials also possess a signal at 0 ppm that remained to be assigned. **††

** Chemical shifts of phosphate esters can vary significantly depending on: (1) the number and electronic characteristics of attached aryl groups; (2) the particular phosphorus environment (mono-, di-, and tri-ester); and (3) the geometry of the O-P-O bond (acyclic, cyclic 5-membered or 6-membered rings). See D. G. Gorenstein, *Phosphorus-31 NMR: Principles and Applications*, Academic Press, Inc., Orlando, 1984.

$\dagger\dagger$ These signals could also be attributed to condensed pyrophosphates having resonances at ca. -20 ppm, or short-chain polyphosphates with middle versus terminal groups typically appearing at -10 and -6 ppm. See ref. 22.

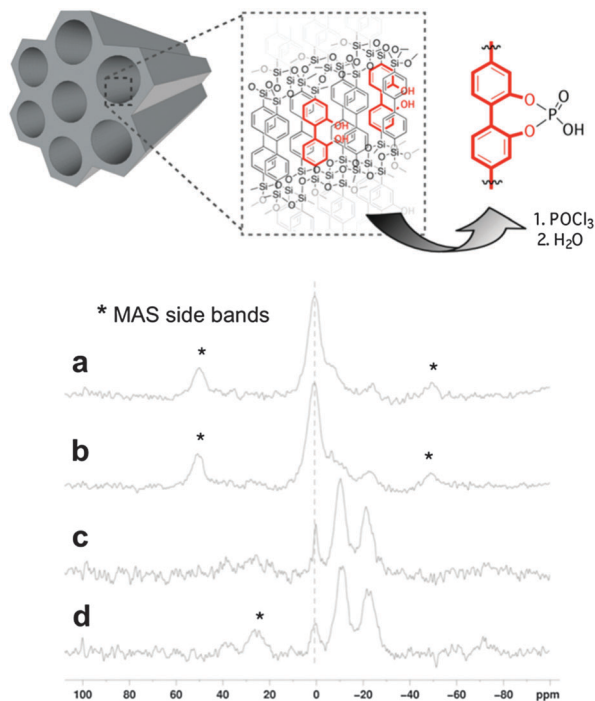


Fig. 6 Solid-state ^{31}P CP MAS NMR spectra of final composite PMO materials obtained by treating the following starting cPMO materials with phosphoryl chloride at room temperature for 18 h: (a) HO-cPMO prepared from $^{20}\text{MEMO}$ -cPMO; (b) HO-cPMO prepared from ^{20}MeO -cPMO; (c) ^{20}MeO -cPMO, and (d) BTESBp-PMO.

A phosphorylated MCM derivative HOP(O)-MCM was prepared by treating MCM-41 with phosphoryl chloride then quenching with water. Since MCM-41 is purely siliceous, all phosphorous species observed on the surface should be derived from silanols. These materials also showed a similar ^{31}P NMR profile to the treated MeO- and BTESBp-PMOs, supporting our interpretation that the signals at -10 and -22 ppm likely originate from surface Si-O-P phosphate esters (Fig. S5, ESI[†] and Fig. 7b),^{‡‡} and they also possess a signal at 0 ppm.

The phosphorylated cPMO and MCM materials described above were subjected to aqueous acid. Based on the stability of phosphate diesters,^{38,39} biphenyl-diyl phosphate diesters within the HOP(O)-cPMOs should be more resistant to acid-catalyzed hydrolysis than surface silyl phosphate esters. In the event, when HOP(O)-MCM was treated with 2 M HCl for 18 hours, complete hydrolysis of all phosphate species was observed, including the small signal at 0 ppm, as indicated by the total loss of ^{31}P signals in the solid-state NMR spectrum (Fig. 7b). However, when PMO-derived material HOP(O)-cPMO, was treated with 2 M HCl under the same conditions, the ^{31}P NMR spectrum showed no apparent loss of the signal at 0 ppm while the signals at -10 and -22 ppm were substantially decreased (Fig. 7c). Removal of the signal at -10 ppm after the acid treatment revealed a small, sharp signal at -6 ppm.

These results indicate that HOP(O)-cPMOs and POCl_3 -treated non-diol materials share a set of signals originating

^{‡‡} The absence of terminal phosphate resonances at -6 ppm also confirmed that these signals do not originate from polyphosphate species.

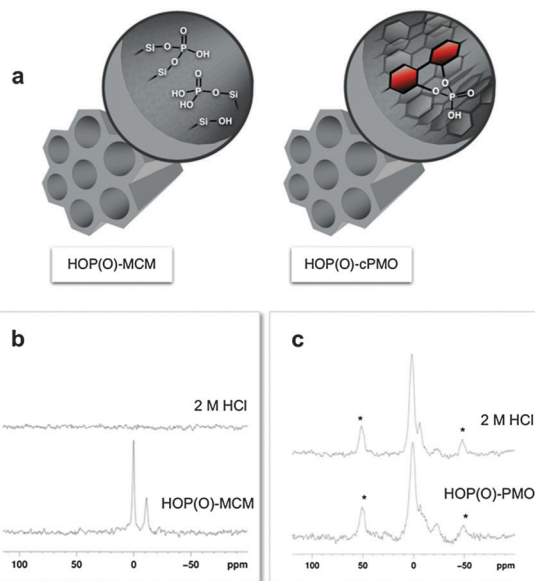


Fig. 7 (a) Comparison of phosphate diester species within HOP(O)-cPMOs versus surface species in MCM materials; and solid-state ^{31}P CP MAS NMR spectra of HOP(O) materials prepared from (b) MCM-41 or (c) HO-cPMO, before and after treatment with 2 M HCl acid, with MAS side-bands indicated by an asterisk (*).

from surface phosphate ester species. However, signals at 0 ppm in the two sets of materials must arise from different species, with HOP(O)-cPMOs revealing an acid-resistant species compared to the acid-susceptible surface phosphoric acid in the latter materials. The acid-resistant phosphate species resonating at -6 ppm is attributed to the monoester phosphate resulting from incomplete phosphorylation of the diol.^{§§}

High-field solid state NMR analysis of the HOP(O)-cPMO phosphorus species was employed to confirm the assignment of the large signal at 0 ppm as resulting from the desired aryl phosphate diester. Although ^{31}P - ^{13}C HETCOR NMR was not sensitive enough to detect coupling of the phosphate phosphorus to its attached biphenylene carbon in the solid state, it was possible to observe long-range phosphorus-proton dipolar coupling with the biphenylene protons on the aromatic ring by ^{31}P - ^1H 2D HETCOR NMR experiments on a 900 MHz instrument over several days. Thus, ^{31}P - ^1H 2D HETCOR NMR spectra of a HOP(O)-cPMO powder sample showed long-range coupling of the phosphate species resonating at 0 ppm to the aromatic biphenylene protons appearing as a broad signal centered at 7 ppm (Fig. 8). The ^{31}P - ^1H 2D HETCOR NMR spectrum of commercial BINOL hydrogen phosphate showed similar ^{31}P - ^1H correlation peaks (Fig. S6, ESI[†]).^{¶¶} A weak correlation peak was

^{§§} While we would expect this phosphate monoester to be somewhat susceptible to hydrolysis, the hydrophobicity of the cPMO bridging groups might afford protection to these organophosphate species in comparison to surface silyl phosphate esters.

^{¶¶} The acidic proton was absent in the HOP(O)-cPMO, or perhaps shifted upfield and overlapped by the aromatic signals. The ^1H signal at 4.5 ppm in the HOP(O)-cPMO is thought to arise from water, and residual aliphatic signals from uncleaved OMEM groups or byproducts of the cleavage.

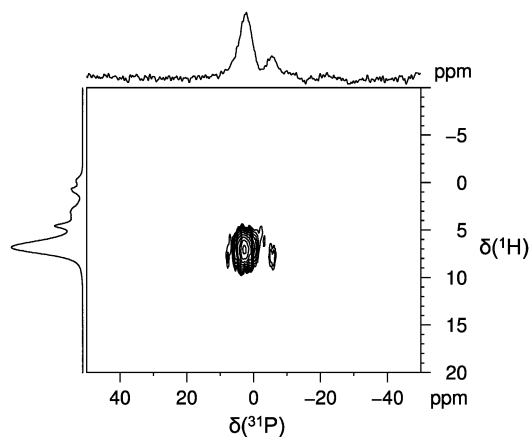


Fig. 8 High-field solid-state ^{31}P - ^1H 2D HETCOR spectrum of HOP(O)-cPMO along with the regular ^{31}P CP MAS (horizontal) and ^1H (vertical) MAS spectra. All spectra were obtained at 21.1 T with a sample spinning of 20 kHz.

also observed between the minor phosphorus signal at -6 ppm and the biphenylene protons of the HOP(O)-cPMO supporting the presence of a biphenyl-diyl monoester phosphate species that would engage in coupling with the neighboring aromatic protons through a single Ar-O-P bond (Fig. 8).

These results are highly encouraging for post-synthetic transformations of functional groups within these types of solid-state materials. They demonstrate that biphenol units liberated by removal of methoxy or MEM groups are accessible within the PMO pore walls and can be transformed by simple chemical manipulation.

Of critical importance, we also showed that small quantities of residual surface-bound species can be easily and selectively removed by acid treatment. We are interested in extending this concept into PMO materials containing chiral functional groups, with the idea that selective manipulation of different diol groups could be realized in a stepwise fashion.

Conclusions

Families of composite periodic mesoporous organosilica materials containing dopant monomers have been prepared that serve as precursors to C_2 -symmetric diol functionality. Biphenylene-bridged materials tolerate the incorporation of functional protected dopants without significant changes to the physical properties of the material. Remarkably, despite the size of the protecting groups, the dopants could be incorporated into the PMO without affecting the long-range order of the organosilica scaffold. Deprotection of the methoxy or methoxyethoxymethyl ether groups within the composite PMO was readily achieved, liberating the free diol that could then be quantitatively transformed into an organophosphate moiety. Although phosphate groups were also incorporated by reaction with simple silanols, these species were easily and selectively removed by acid treatment. This lays important ground-work for the preparation of complex hybrid periodic mesoporous organosilicas for catalysis and other advanced applications.

Acknowledgements

The authors thank the Natural Sciences and Engineering Research Council (NSERC) for support through the Chiral Materials Collaborative Research and Training Experience (CREATE) Program. C. M. C thanks NSERC for Discovery and Accelerator awards, as well as the Canada Foundation for Innovation (CFI) for infrastructure awards. L. M. R thanks NSERC, the Marie Mottashed foundation, and the Walter C. Sumner Memorial foundation for awards. Additionally the authors thank Dr Francoise Sauriol (Queen's University) for solid-state NMR analysis, Dr Victor V. Terskikh (High-field NMR Facility, Ottawa) for high-field solid-state NMR analysis, Victoria Jarvis (McMaster University) for XRD analysis, and Dr Louise Weaver (University of New Brunswick) for TEM analysis.

Notes and references

- 1 F. Hoffmann, M. Cornelius, J. Morell and M. Fröba, *Angew. Chem., Int. Ed.*, 2006, **45**, 3216–3251.
- 2 F. Hoffmann and M. Fröba, *Chem. Soc. Rev.*, 2011, **40**, 608–620.
- 3 N. Mizoshita, T. Tani and S. Inagaki, *Chem. Soc. Rev.*, 2011, **40**, 789–800.
- 4 P. Van Der Voort, D. Esquivel, E. De Canck, F. Goethals, I. Van Driessche and F. J. Romero-Salguero, *Chem. Soc. Rev.*, 2013, **42**, 3913–3955.
- 5 C. Chen, L. Kong, T. Cheng, R. Jin and G. Liu, *Chem. Commun.*, 2014, **50**, 10891–10893.
- 6 K. Nakajima, I. Tomita, M. Hara, S. Hayashi, K. Domen and J. N. Kondo, *Adv. Mater.*, 2005, **17**, 1839–1842.
- 7 D. Esquivel, E. De Canck, C. Jiménez-Sanchidrián, P. Van Der Voort and F. J. Romero-Salguero, *J. Mater. Chem.*, 2011, **21**, 10990–10998.
- 8 J. Ouwehand, J. Lauwaert, D. Esquivel, K. Hendrickx, V. Van Speybroeck, J. W. Thybaut and P. Van Der Voort, *Eur. J. Inorg. Chem.*, 2016, **13–14**, 2144–2151.
- 9 D. Dubé, M. Rat, F. Béland and S. Kaliaguine, *Microporous Mesoporous Mater.*, 2008, **111**, 596–603.
- 10 M. Ohashi, M. P. Kapoor and S. Inagaki, *Chem. Commun.*, 2008, 841–843.
- 11 M. A. O. Lourenço, J. R. B. Gomes and P. Ferreira, *RSC Adv.*, 2015, **5**, 9208–9216.
- 12 S. Inagaki, S. Guan, T. Ohsuna and O. Terasaki, *Nature*, 2002, **416**, 304–307.
- 13 D. Esquivel, C. Jiménez-Sanchidrián and F. J. Romero-Salguero, *J. Mater. Chem.*, 2011, **21**, 724–733.
- 14 M. Beretta, J. Morell, P. Sozzani and M. Fröba, *Chem. Commun.*, 2010, **46**, 2495–2497.
- 15 M. A. O. Lourenço, R. Siegel, L. Mafra and P. Ferreira, *Dalton Trans.*, 2013, **42**, 5631–5634.
- 16 M. P. Kapoor, Q. Yang, Y. Goto and S. Inagaki, *Chem. Lett.*, 2003, **32**, 914–915.
- 17 C. He, P. Liu, P. J. McMullan and A. C. Griffin, *Phys. Status Solidi B*, 2005, **242**, 576–584.

- 18 M. P. Kapoor, Q. Yang and S. Inagaki, *J. Am. Chem. Soc.*, 2002, **124**, 15176–15177.
- 19 X. Liu, P. Wang, L. Zhang, J. Yang, C. Li and Q. Yang, *Chem. – Eur. J.*, 2010, **16**, 12727–12735.
- 20 J. M. Brunel, *Chem. Rev.*, 2007, **107**, PR1–PR45.
- 21 Y. Chen, S. Yekta and A. K. Yudin, *Chem. Rev.*, 2003, **103**, 3155–3212.
- 22 S. J. Connon, *Angew. Chem., Int. Ed.*, 2006, **45**, 3909–3912.
- 23 M. Murata, H. Yamasaki, T. Ueta, M. Nagata, M. Ishikura, S. Watanabe and Y. Masuda, *Tetrahedron*, 2007, **63**, 4087–4094.
- 24 J. F. W. McOmie, M. L. Watts and D. E. West, *Tetrahedron*, 1968, **24**, 2289–2292.
- 25 P. Wang, J. Yang, J. Liu, L. Zhang and Q. Yang, *Microporous Mesoporous Mater.*, 2009, **117**, 91–97.
- 26 A. Roussey, D. Gajan, T. K. Maishal, A. Mukerjee, L. Veyre, A. Lesage, L. Emsley, C. Copéret and C. Thieuleux, *Phys. Chem. Chem. Phys.*, 2011, **13**, 4230–4233.
- 27 X. Liu, P. Wang, Y. Yang, P. Wang and Q. Yang, *Chem. – Asian J.*, 2010, **5**, 1232–1239.
- 28 D. Uraguchi and M. Terada, *J. Am. Chem. Soc.*, 2004, **126**, 5356–5357.
- 29 E. G. Gutierrez, E. J. Moorhead, E. H. Smith, V. Lin, L. K. G. Ackerman, C. E. Knezevic, V. Sun, S. Grant and A. G. Wenzel, *Eur. J. Org. Chem.*, 2010, 3027–3031.
- 30 K. Mori, K. Ehara, K. Kurihara and T. Akiyama, *J. Am. Chem. Soc.*, 2011, **133**, 6166–6169.
- 31 K. Makiguchi, T. Yamanaka, T. Kakuchi, M. Terada and T. Satoh, *Chem. Commun.*, 2014, **50**, 2883–2885.
- 32 A. Alexakis and C. Benhaim, *Eur. J. Org. Chem.*, 2002, 3221–3236.
- 33 C. Monti, C. Gennari, U. Piarulli, J. G. de Vries, A. H. M. de Vries and L. Lefort, *Chem. – Eur. J.*, 2005, **11**, 6701–6717.
- 34 J. Zhuang, D. Ma, G. Yang, Z. Yan, X. Liu, X. Liu, X. Han, X. Bao, P. Xie and Z. Liu, *J. Catal.*, 2004, **228**, 234–242.
- 35 C. Coelho, F. Babonneau, T. Azaïs, L. Bonhomme-Coury, J. Maquet, G. Laurent and C. Bonhomme, *J. Sol-Gel Sci. Technol.*, 2006, **40**, 181–189.
- 36 S. Jähnigen, E. Brendler, U. Böhme, G. Heide and E. Kroke, *New J. Chem.*, 2014, **38**, 744–751.
- 37 A. Styskalik, D. Skoda, Z. Moravec, P. Roupčova, C. E. Barnes and J. Pinkas, *RSC Adv.*, 2015, **5**, 73670–73676.
- 38 A. J. Kirby and M. Younas, *J. Chem. Soc. B*, 1970, 510–513.
- 39 J. Kumamoto and F. H. Westheimer, *J. Am. Chem. Soc.*, 1955, **77**, 2515–2518.